On-Bead Combinatorial Synthesis and Imaging of Chemical Exchange Saturation Transfer Magnetic Resonance Imaging Agents To Identify Factors That Influence Water Exchange

Roberta Napolitano,[†] Todd C. Soesbe,[†] Luis M. De León-Rodríguez,[†,§] A. Dean Sherry,[†,‖] and D. Gomika Udugamasooriya*,[†,‡]

[†]Advanced Imaging Research Center and [‡]Department of Biochemistry, University of Texas Southwestern Medical Center, 5323 Harry Hines Boulevard, Dallas, Texas 75390-8568, United States

[§]Departamento de Química, Universidad de Guanajuato, Cerro de la Venada s/n, Guanajuato, Gto. 36040, Mexico

[‖]Department of Chemistry, University of Texas at Dallas, 800 West Campbell Road, Richardson, Texas 75083-3021, United States

Ⓢ Supporting Information

ABSTRACT:
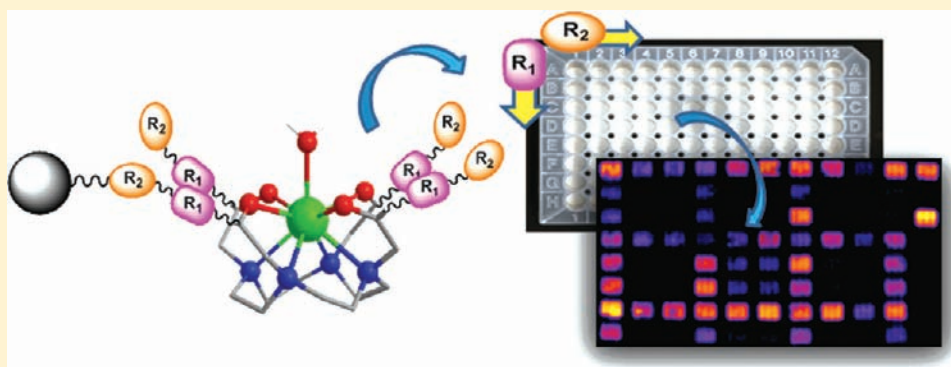
The sensitivity of magnetic resonance imaging (MRI) contrast agents is highly dependent on the rate of water exchange between the inner sphere of a paramagnetic ion and bulk water. Normally, identifying a paramagnetic complex that has optimal water exchange kinetics is done by synthesizing and testing one compound at a time. We report here a rapid, economical on-bead combinatorial synthesis of a library of imaging agents. Eighty different 1,4,7,10-tetraazacyclododecan-1,4,7,10-tetraacetic acid (DOTA)-tetraamide peptoid derivatives were prepared on beads using a variety of charged, uncharged but polar, hydrophobic, and variably sized primary amines. A single chemical exchange saturation transfer image of the on-bead library easily distinguished those compounds having the most favorable water exchange kinetics. This combinatorial approach will allow rapid screening of libraries of imaging agents to identify the chemical characteristics of a ligand that yield the most sensitive imaging agents. This technique could be automated and readily adapted to other types of MRI or magnetic resonance/positron emission tomography agents as well.

■ INTRODUCTION

Magnetic resonance imaging (MRI) is one of the most important diagnostic imaging tools in clinical medicine today. Exogenous paramagnetic metal complexes are often used as contrast agents to shorten the relaxation times of the water protons and thereby enhance tissue contrast in regions where such agents accumulate. Over the past few years, new methods have been explored for introducing image contrast,[1] including those based on chemical exchange saturation transfer (CEST) mechanisms.[2−11] Briefly, CEST contrast arises as a result of selective saturation (through application of a suitable radio-frequency field) of a proton pool that is in slow-to-intermediate exchange with bulk water protons. Chemical transfer of those saturated spins originally on the agent into the water pool results in a decrease in the measured water signal, hence a darkening of the image. Originally, the attention was focused on protons from small diamagnetic molecules with −NH and −OH protons in exchange with bulk water.[8,12,13] However, the chemical shift difference between the exchanging protons and bulk water in such diamagnetic CEST agents is typically <5 ppm. This makes it technically more difficult to saturate one proton pool without inadvertently also partially affecting the other as well. One advantage of using paramagnetic lanthanide complexes as CEST agents (PARACEST) is that the chemical shift difference between the two exchangeable pools can be increased substantially.
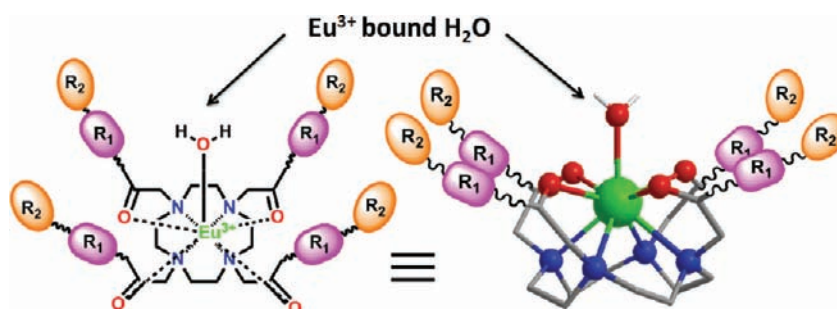
Figure 1. Schematic representation of a Eu[III]DOTA-based PARACEST agent where the position of the Eu(III)-bound water molecule is shown (arrows). The exchange kinetics of this water molecule with bulk water is modulated by the surrounding ligands on the four arms of the DOTA scaffold (e.g., R_1 and R_2 represent the two peptoid residues that build diversity into the combinatorial library developed in this study).

For example, a slowly exchanging bound water resonance near 50 ppm is often seen in CEST spectra of Eu-1,4,7,10-tetraazacyclo-dodecan-1,4,7,10-tetraacetic acid-tetraamide (EuDOTA-tetra-amide) complexes such as those shown in Figure 1.[7] This makes it easy to selectively saturate this exchanging pool without affecting the bulk water signal.[8] PARACEST agents such as these have some potential advantages over the more conventional T_1 and T_2 relaxation agents because image contrast is under operator control and can be turned on and off at will.[8] A second advantage is that the CEST signal produced by EuDOTA-tetraamide complexes is quite sensitive to the rate of water molecule exchange between the inner sphere of the Eu(III) coordination site and bulk water.[14] This makes it easy to design responsive agents that alter this rate by ligand electronic effects, stereo-chemistry, and polarity of the neighboring substituents [Figure 1(R_1 and R_2)].[6] The primary disadvantage of current PARACEST agents is their low sensitivity compared to that of conventional T_1 and T_2 agents.[5]

Previous experiments have shown that a complex interplay of chemical factors contribute to water exchange in these complexes and that CEST sensitivity may be improved substantially by dramatically slowing the rate of water exchange in these complexes.[6] However, it is a difficult challenge to understand how all these possible parameters collectively influence the CEST signal by synthesizing and studying one agent at a time, the usual approach. Also, this is a major limitation in identifying the optimal PARACEST agents using this time-consuming conventional solution-phase synthesis and MRI analysis. For this reason, we have been exploring the possibility of introducing a large number of chemical variables into the basic DOTA scaffold using on-bead combinatorial chemical methods in an effort to directly identify those chemical features that yield optimal water exchange rates for CEST imaging. The advantages of collecting a single CEST image of a small library of polypeptides in solution have been demonstrated previously.[15,16] Here, we report (i) a rapid, convenient on-bead synthesis of a library of 80 different PARACEST agents that differ only in the chemical identity of side arms on the DOTA scaffold [Figure 1(R_1 and R_2)] and (ii) a method for simultaneous CEST imaging of the entire library without removal of the agents from the beads. The resulting images provide a direct readout of those structures that display the best water exchange properties for CEST imaging.

■ EXPERIMENTAL METHODS

On-Bead Bulk Synthesis of Parent Compound 16. TentaGel macrobeads were placed in five peptide reaction vessels (total 1 g,

200 mg/vessel), swelled in N,N-Dimethylformamide (DMF), and treated with Fmoc-Met-OH, O-Benzotriazole-N,N,N′,N′-tetramethyl-uronium-hexafluoro-phosphate (HBTU) and 4-Methylmorpholine (NMM) in DMF overnight. After the beads were washed with DMF, the Fmoc group was removed (20% piperidine in DMF). The peptoid portion (two methoxyethylamine units) was added using a two-step (bromoacetylation and methoxyethylamine substitution) microwave-assisted synthesis protocol [10% power (2 × 15 s)] as previously reported.[17] Then Fmoc-β-Ala-OH was coupled as described above for the methionine coupling. After removal of the Fmoc group, the beads were treated with bromoacetic acid/N,N-Diisopropylcarbodiimide (DIC) in the microwave oven at 10% power (2 × 15 s). The beads were then treated with 1 M 1,4,7,10-tetraazacyclododecan-1,4,7-triacetic acid-tris(tert-butyl ester) solution in the microwave oven at 10% power (3 × 15 s). After the beads were washed with DMF and Dichloromethane (DCM), the tert-butyl groups were removed (95% TFA, 2.5% triisopropylsilane, and 2.5% water, 4 h). After being washed with DCM and DMF, the beads were treated with N-Boc-1,2-diaminoethane, HBTU, and NMM for 24 h. Finally, the Boc group was removed as described above using 95% TFA.

Synthesis of the Library. The library was synthesized starting from the parent compound **16** (Scheme 2) and adding two peptoid moieties onto each of the three free arms of the DOTA scaffold. Bromoacetic acid coupling of the first peptoid residue was performed in bulk synthesis. Then the beads were equally (∼10 mg/well) distributed into a 96-AcroWell filter plate (PALL). The first eight amines (Chart 1; some were protected accordingly) were added (2 M, 180 μL/well) to each row of the plate (shaking for 2 h, 250 rpm). After DMF washing by centrifugation, bromoacetic acid/DIC was added for 30 min twice (shaking for 2 h, 250 rpm). After DMF washing, 10 amines (Chart 1) were added to each of the first 10 columns of the plate. Beads containing β-alanine and 1,2-diaminoethane were transferred to another TFA-resistant 96-well plate, treated with a 95% TFA, 2.5% triisopro-pylsilane, and 2.5% water mixture for 4 h to remove tert-butyl and the Boc protection group. The beads were washed with DCM and DMF, finally neutralized with 20% piperidine in DMF for 5 min, and transferred to the previous plate. All wells were washed with water and allowed to swell in water for 1 h. The metal complexation was performed with a 0.2 M EuCl₃ solution at pH 6.3 overnight. Finally, the beads were washed with water (5×), dried, and stored at 4 °C.

Cleavage, Purification, and Mass Analysis. The cyanogen bromide cleavage[18] was used to confirm the synthesis of each step up to compound **16** and then for the 10 representative compounds of the library. The beads were treated with the cleavage solution (0.28 M CNBr in a 5:4:1 acetonitrile/acetic acid/water mixture) overnight. CNBr and acetic acid were removed under a nitrogen flow. The residue was redissolved in a 1:1 acetonitrile/water mixture for mass and HPLC analysis.

Chart 1. Structures of the 10 Primary Amines Used To Build the Library
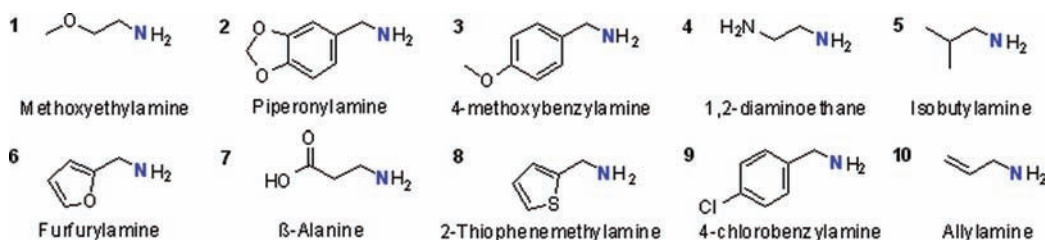
Scheme 1. Two Basic Peptoid Synthesis Steps Carried Out on a Bead-Attached DOTA Scaffold Adding One Peptoid Residue
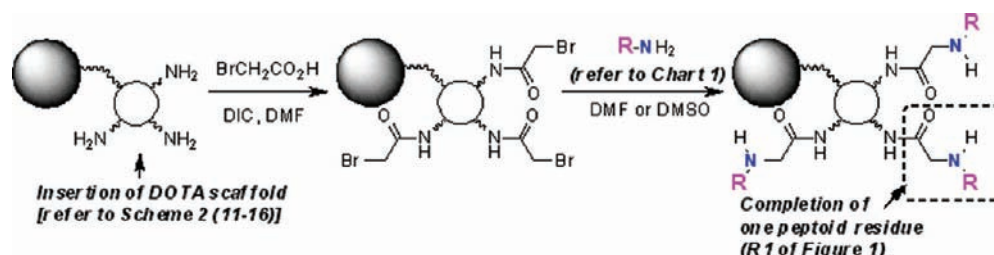
NMR. CEST spectra were collected on beads placed in 3 mm NMR tubes filled with water using a Varian 9.4 T NMR system with the sample temperature maintained at 25 °C. A B1 of 300 Hz and 5 s duration was applied at each frequency prior to collection of a ^{1}H spectrum of water.

CEST Imaging of the Library. In vitro imaging was performed on a Varian 9.4 T animal system using a 63 mm diameter quadrature volume coil. The samples were placed at the gradient isocenter with the temperature maintained at 20 °C using warmed air and a thermocouple. A single coronal plane ($64 \times 64 \times 2$ mm) passing through the bottom portion of each sample well was selected for imaging. Image-based CEST spectra acquired with the fast spin−echo sequence (TR/TE = 69.8 ms/8.4 ms, echo train 8, averages 2, $64 \times 64 \times 1$ pixel matrix) were used to measure the CEST frequency ($\Delta\omega$) for each well. Images were then acquired using the fast spin−echo sequence (TR/TE = 69.8 ms/8.4 ms, echo train 8, averages 2, $64 \times 64 \times 1$ pixel matrix) with saturation at both +50 ppm ("on") and −50 ppm ("off"). A 5 s long, 10 μT saturation pulse was used for every TR. A CEST image was created by subtracting the two images (off − on). Spatial susceptibility effects within the samples were minimized using two methods. First, the 8×11 sample wells were surrounded by a two-well thick boarder of pure water. Second, after the first set of images was taken, the sample was rotated by 180° and imaged again. The two CEST images at 0° and 180° were then averaged. These methods assured that the CEST variations from well to well were due to changes in chemical configuration and not susceptibility effects.

Eu(III) Quantitative Assay. Ten beads from each of the individual wells selected were isolated and collected in Eppendorf tubes. A 2.0 M solution of HCl (50 μL/tube) was added and incubated at 37 °C for 2 h. Then the samples were neutralized using 2.0 M NaOH (55 μL/tube). The enhancement solution was added (115 μL/tube) and incubated for 30 min at 37 °C. Fluorescence emission at 615 nm was detected using a SpectraMax M5 spectrophotometer.

■ RESULTS AND DISCUSSION

The solid-phase synthesis strategy was to (i) attach a DOTA scaffold to TentaGel macrobeads (300 μm diameter) through a linker to a single carboxyl group, (ii) couple ethylenediamine to the remaining three carboxyl groups of DOTA to provide terminal amines for building the library, and (iii) add two rounds of "peptoid" monomers to the three free primary amino groups to create the ligand library. Peptoids were selected as the diversity component [Figure 1(R_1 and R_2)] because the chemistry is simple and fast and many primary amines are available that would introduce a variety of chemical properties into the ligand side arms (hydrophobicity, size, charge). The well-established on-bead peptoid synthesis is based on simple two-step chemical reactions, an acylation step using diimide-activated bromoacetic acid followed by nucleophilic displacement of the bromide with a primary amine (Scheme 1).[19] These reactions are not air sensitive or particularly moisture sensitive and typically take place in high yield at each step. Thus, the entire process can be automated, adapted to most commercial peptide synthesizers, and even accelerated to less than 1 min using microwave irradiation.[17] The amines chosen for the library provided variable charge, polarity, and steric bulkiness around the Eu(III)−water exchange site (Chart 1). The blue-colored nitrogen atom in each amine (Chart 1) will be incorporated into the peptoid backbone (see Scheme 1, second step), leaving the remaining portion as the "R" group.

The synthesis scheme is shown in Scheme 2. The initial common synthetic steps (steps 11−16, Scheme 2) were carried out in bulk using standard glassware, while the remaining diverse regions (steps 17 and 18, Scheme 2) were carried out using a 96-well synthesis filter plate [Scheme 2 (inset)]. First, a spacer between the bead and the DOTA scaffold was introduced. Methionine was added as the first residue of the spacer arm so the final product could be cleaved from the resin with cyanogen bromide for subsequent mass spectroscopic confirmation. To obtain reasonably symmetrical DOTA-tetraamide products and to limit possible steric hindrance between the EuDOTA complex and the bead surface, two neutral methoxyethylamine moieties were added next. Here, both the bromoacetic acid addition and amine coupling reactions were assisted by microwave irradiation.[17,19] Then

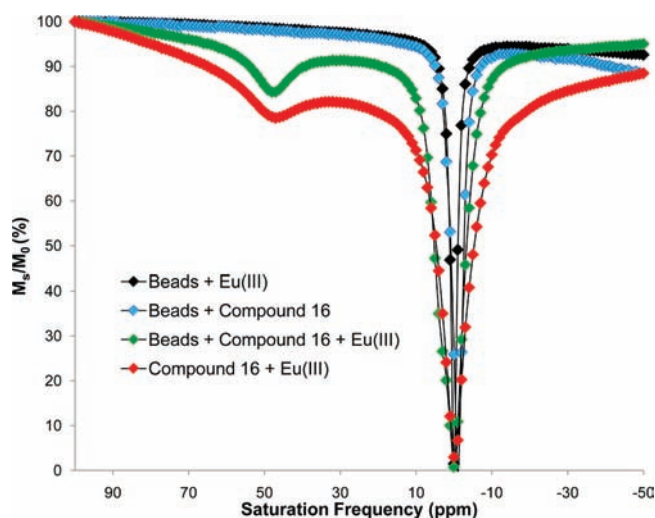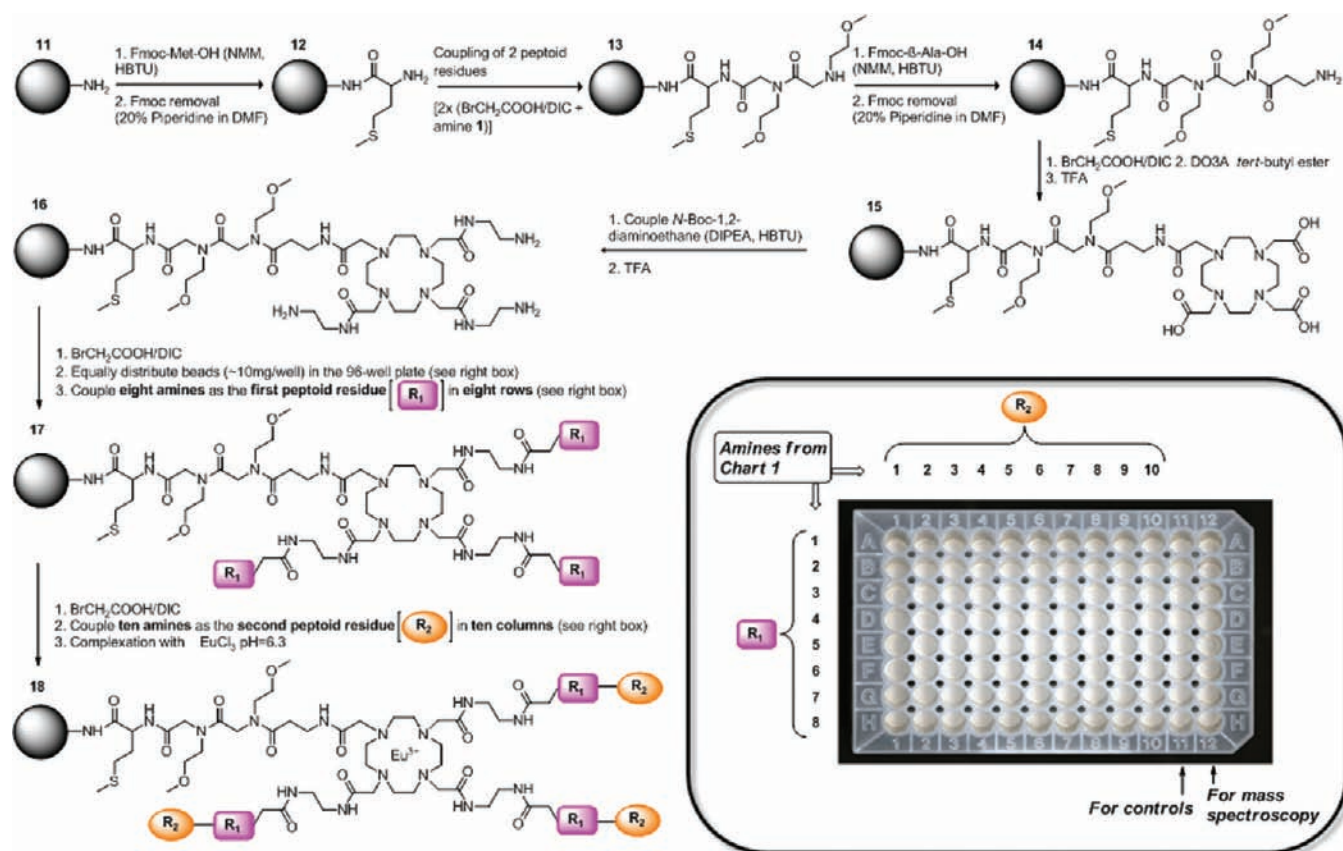**Scheme 2. Flow Chart of the Complete Library Synthesis**

Figure 2. Comparison of Z-spectra of **Eu*16** attached to beads with different controls [**Eu*16** attached to beads, **Eu*16** in solution without the beads, beads alone (no **16**, but treated with Eu(III)), or beads with ligand **16** but no added Eu(III)].

β-alanine was added to mimic the ethylenediamine spacer planned for the other three DOTA arms, and finally DO3A *tert*-butyl ester was coupled. The three remaining carboxyl groups of DOTA were then reacted with monoprotected 1,2-diaminoethane

(step 15 and 16, Scheme 2) to yield **16**, the starting material for building the peptoid library.

A critical test was carried out at this point to verify that resin-bound DOTA-tetraamide forms a complex with Eu(III) and to test whether a CEST signal could be detected with the EuDOTA-tetraamide complex bound to the beads. Eu(III) complexation was performed by addition of ~15-fold excess EuCl$_3$ at pH 6.3 overnight, followed by removal of excess Eu(III) by washing the resin several times with water. A few beads were then removed and placed in a glass capillary for collection of a CEST spectrum using a vertical bore 400 MHz NMR spectrometer. Importantly, a large Eu(III)-bound water exchange peak was observed in the CEST spectrum near 50 ppm (Figure 2, green data points). No CEST was observed for ligand **16** alone [no Eu(III)] or empty beads treated with EuCl$_3$, confirming that the CEST signal reflects **Eu*16** attached to the beads (Figure 2, blue and black data points). The CEST signal of a solution of **Eu*16** after it was cleaved from the beads (see section S2, Supporting Information) displayed a chemical shift similar to that of the bead-bound complex, but the exchange peak was slightly broader (Figure 2, red data points). This implies that water exchange may be somewhat slower for the complex attached to beads, although absolute comparisons of exchange rates were not possible because the concentrations of the two samples were unknown. Most importantly, these data show that the CEST signal from a covalently attached complex (**Eu*16**) is not strongly influenced by the presence of the Tentagel beads. This observation allowed us to proceed with the synthesis of a diverse chemical library of
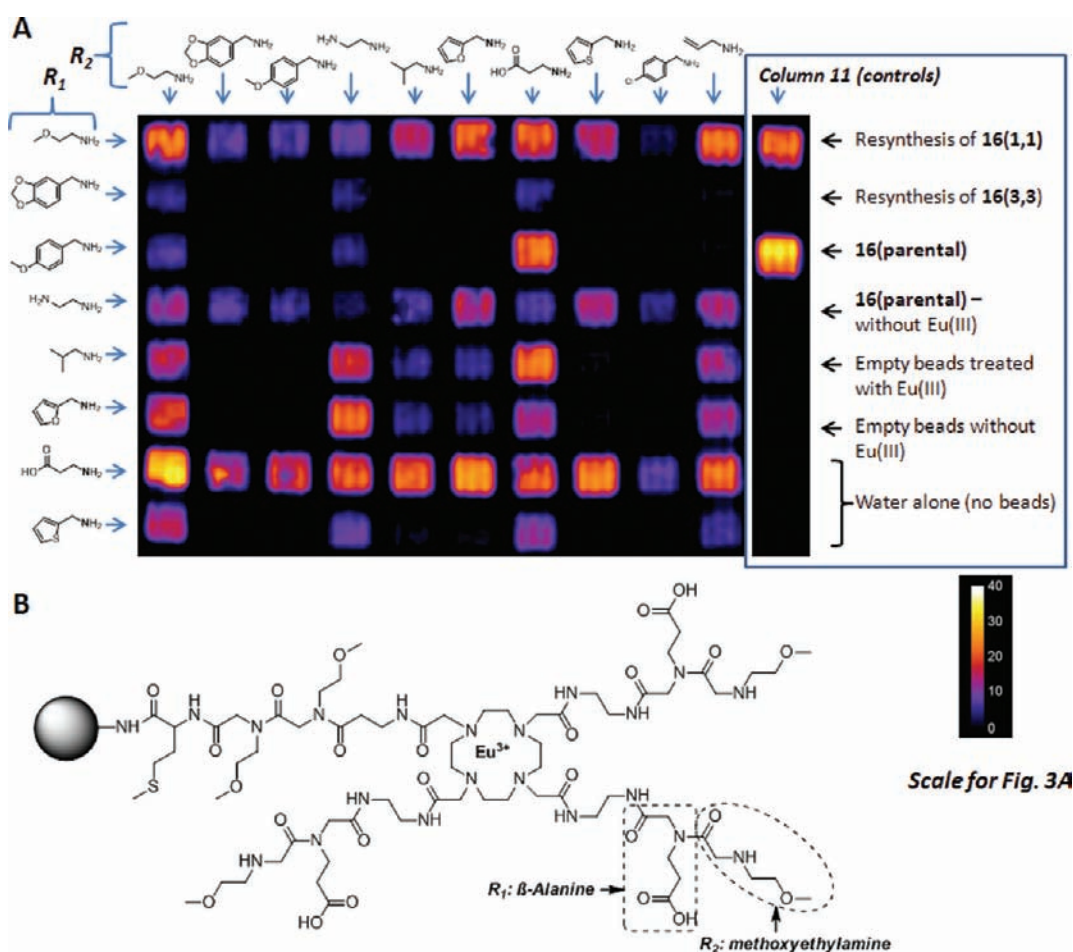
Figure 3. (A) CEST image of the 80-compound library of Eu^{III}DOTA-tetraamide peptoid derivatives attached to beads. The color scale displays the percent change in bulk water intensity $(1 - M_s/M_o)$ with a presaturation pulse set either off resonance (M_o) or on resonance (M_s). The chemical structures of each amine used to build the library are shown along each horizontal row (R_1) and each vertical column (R_2). A number of control samples were located in column 11, identified as indicated in the figure. (B) Structure of the Eu^{III}DOTA-tetraamide peptoid (bead-attached form) in well (7, 1) that showed the highest CEST intensity.

CEST ligands, including hydrophobic side arms that might not ordinarily be soluble when prepared in bulk.

The parallel combinatorial synthesis approach was used to couple two peptoid residues onto **16**. Bromoacetic acid was coupled (for the first peptoid residue) to **16** in bulk before the beads were distributed equally into a 96-well synthesis plate [Scheme 2 (inset)]. To avoid possible inhomogeneous microwave irradiation in the different wells of the plate, the remaining peptoid coupling steps were performed for an extended period of time at room temperature.[17] The first eight rows and ten columns were used for synthesis of the library; column 11 was used for controls, and column 12 was used for synthesis of eight additional DOTA-tetraamide peptoids using random combinations of amines (see section S3, Supporting Information) for cleavage and mass spectroscopy analyses.

Eight different amines (**1**−**8**, Chart 1) were coupled to the three remaining arms of DOTA to complete the first residue in each row [i.e., R_1 in row 1 was methoxyethylamine (**1**), R_1 in row 2 was piperonylamine (**2**), R_1 in row 3 was 4-methoxybenzyla-mine (**3**), etc]. This was followed by a second bromoacetic acid coupling step to prepare for the second amine. Amines **1**−**10** (Chart 1) were chosen as residue R_2; **1** was added to each of eight wells in column 1, **2** was added to each of eight wells in column 2,

etc. to yield an array of compounds having the same first peptoid along each row ($R_1 = $ **1**−**8**) and the same second residue along each column ($R_2 = $ **1**−**10**). This simple approach allowed rapid access to $8 \times 10 = 80$ different compounds, all built on the same parental DOTA-tetraamide scaffold and differing only in the chemical identity of R_1 and R_2. Finally, Eu(III) complexation was performed as described previously. Before proceeding with the MRI measurements, the quality of the library was checked by analyzing the representative compounds synthesized in the 12th column using MALDI-TOF MS to confirm the complete synthesis of all eight compounds (see section S3, Supporting Information). Random samples were not withdrawn from the actual 80-compound library for this purpose to have the same number of beads in each well for imaging.

To register a single image for all 80 compounds plus controls, the beads were first transferred from the synthesis/filtration plate to the central 80 wells of a 145-well plate to maximize the height of the packed beads in the 4 mm diameter well. All 145 wells were filled with water, including those on the perimeter that did not contain beads, to make the sample as homogeneous as possible. The plate was then positioned in the center of a 63 mm quadrature volume coil, and CEST imaging was performed by applying a $10\,\mu$T frequency-selective presaturation pulse for 5 s followed by

a spin—echo sequence using a 9.4 T Varian scanner. A 2 mm thick coronal slice was selected near the bottom of each well to ensure that each image would reflect an equal number of beads (the height of packed beads in each well was >3 mm). The resulting CEST image (Figure 3) is defined as the difference in water intensities in an image collected with the presaturation pulse set to −50 ppm (control) minus a second image collected with the presaturation pulse set to +50 ppm. This experiment was repeated on another day, and the same image was obtained, thereby confirming the reproducibility of this library imaging experiment.

After the plate was imaged, 10 beads were collected from each of 11 wells selected from those that showed large variations in CEST signal intensities that include empty beads and beads from the well containing **Eu*16**. These beads were treated with HCl to displace all Eu(III) from each chelate and analyzed for total Eu(III) using a commercially available fluorescence enhance-
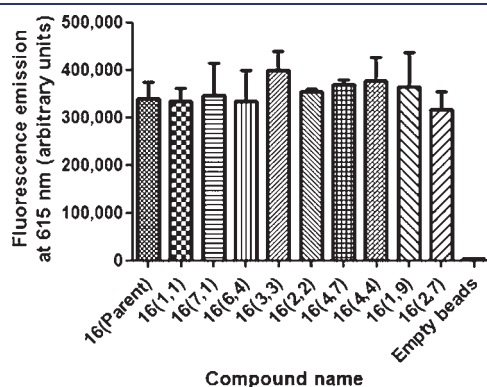

Figure 4. Eu(III) quantification of 10 beads collected from each of 11 wells (as identified below each column).

ment assay.[20,21] These data (Figure 4) indicated that there was an identical amount of total Eu(III) in each 10-bead sample and that empty beads treated with Eu(III) did not retain a significant amount of ion. Thus, any intensity differences in the CEST images shown in Figure 3 could be attributed solely to consequences of the chemical differences of the side arms in the 80 different EuDOTA-tetraamide complexes and not differences in agent concentrations.

The resulting CEST image (Figure 3) illustrates the power of the technique; the CEST signal in some wells was quite intense (up to a 30% reduction in water intensity), while little to no CEST was detected in other wells. To check whether this may be due to frequency differences in the exchanging Eu(III)-bound water resonance in each complex and to show that the spectra were consistent with the imaging data, complete CEST spectra were collected on several individual wells (Figure 5). For those wells showing a CEST signal, the Eu(III)-bound water exchange peak appeared between 50 and 51 ppm (Figure 5) in all cases. The quantitative percent CEST signal $(1 - (M_{(+50)}/M_{(-50)} \times 100)$ from each well varied from 0 to 25% (Table 1, Supporting Information) and was consistent with the qualitative image intensities shown in Figure 3. The most intriguing part of the study came from a comparison of the combined effects of various physicochemical properties of R_1 and R_2 on water exchange at each Eu(III) center.

The most intense CEST signals came from wells containing Eu(III) complexes with small ether, polar, or charged residues such as methoxyethyl (**1**), carboxyethyl (**7**), or the furans (**6** and **8**) [compounds in wells (1, 1), (1, 6), (1, 7), (7, 1), (7, 6), (7, 7), and (7, 8), where the designation (R_1, R_2) refers to (row, column), Figure 3A]. Interestingly, the position of each residue also had consequences on the CEST signal intensity. A more intense CEST signal was seen when a carboxyethyl group (**7**) was
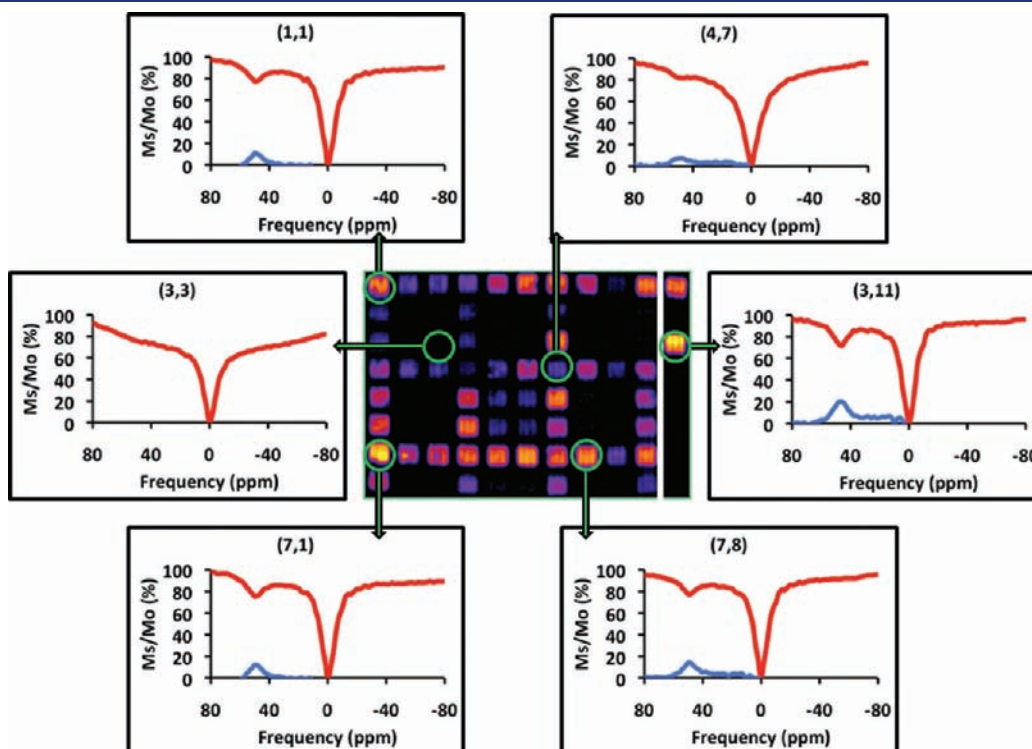

Figure 5. On bead CEST spectra collected from six selected wells of the library. CEST spectra are shown in red and the quantitative percent CEST signal is shown in blue.

the first residue (almost independent of which residue was present at the second position; see row 7) compared to when it was the second residue (column 7). For example, equally intense CEST signals were seen for compounds containing the carboxyethyl group (**7**) in the first peptoid position and either 2-methylfuran (7, 6) or 2-methylthiophene (7, 8) in the second position, but when the sequence was inverted [(6, 7) and (8, 7)], both resulted in a weak CEST signal. Thus, one can conclude that the presence of a negatively charged group in the peptoid positioned closest to the Eu(III) center has a positive influence on the CEST signal. This is consistent with previous data reporting that EuDOTA-tetraglycinate has one of the slowest water exchange rates of any CEST agent reported to date.[22] The opposite trend was seen for the positively charged aminoethyl group (**4**). Here, the CEST intensities did depend on the identity of the second group, but in general, a larger CEST signal was seen for those compounds where the positively charged group (**4**) occupied the second position of the peptoid sequence, not the first (compare the three bright signals in column 4 with the virtually all dark signals in row 4). This was highlighted even further for those compounds having one positively and one negatively charged group together in one sequence; in this case, as usual, the best CEST signal was found for those compounds with the negatively charged carboxyethyl group (**7**) closest to the metal center (7, 4). When the positively charged aminoethyl group (**4**) occupied the first position, this canceled most of the advantage of having the negatively charged carboxyethyl group in the second position [compare the signal intensity of (4, 7) with that of (3, 7) or (5, 7)]. This suggests that having a nonpolar group close to the metal center is more advantageous than having a positively charged group near the metal center, as long as the second position is occupied by the negatively charged, carboxyethyl group [(1, 7) (3, 7), (5, 7), (6, 7)].

In all cases, the bulkier aromatic groups, 5-benzyl-1,3-dioxole (**2**), 4-methoxybenzyl (**3**), or 4-chlorobenzyl (**9**), resulted in the weakest CEST signals, regardless of their position in the peptoid sequence (compare the number of dark wells in columns 2, 3, 8, and 9 with that in any of the other columns). This is in agreement with our prior observations that bulkier aromatic residues such as these increase the rate of water exchange in EuDOTA-tetraamide complexes.[23] Interestingly, the smaller aliphatic, hydrophobic isobutyl group (**5**) did not show a similar trend. When this group appeared in combination with a carboxyethyl group (in either order), the CEST intensities were similar [compare well (5, 7) with well (7, 5)]. A similar but less obvious trend was observed with 2-methylfuran (**6**) or 2-methylthiophene (**8**) acting as the small nonpolar residue in combination with a charged group (either positive or negative) as the second component [(6, 4), (8, 4), (6, 7), (8, 7)]. This suggests that having a small nonpolar group closest to the Eu(III)—water exchange site may act to slow dissociation of the inner-sphere water molecule from the Eu(III) coordination site while the charged group further away acts to organize second-sphere water molecules to slow their entrance into a position where they can be in a position to exchange with the single, inner-sphere water molecule.

It has been reported that the resonance frequency of the bound water is quite sensitive to the identity of the first amide side chain group in a series of tetrasubstituted amino acids, for example.[24] This did not hold true for the 80 complexes prepared in this library because all four side chains were positioned well away from the central EuDOTA structure by the four ethylenediamine arms. In this case, the frequency of the water exchange peak did not vary substantially (all were near 50−51 ppm) because the ethylenediamine spacer placed the chemically diverse substituents far enough away from the metal to minimize any changes in the ligand field. Nevertheless, the most surprising finding of this study was that the water exchange rate and hence the CEST intensity can vary substantially even with these chemically diverse groups positioned well away from the central Eu(III). Thus, the differences in CEST signal intensities observed here can only reflect differences in water accessibility to the inner-sphere coordination sphere.

The use of peptoids as the diversity component has some advantages for future potential applications. These include rapid and inexpensive synthesis of peptoid libraries.[19,25−28] In addition, peptoids are serum stable,[28,29] more cell permeable,[30] and nonimmunogenic,[31] important considerations for any potential clinical application.

■ CONCLUSION

We have presented a combinatorial approach for an easy, rapid, and cost-effective synthesis and screening of a library of possible PARACEST contrast agents by utilizing peptoid chemistry and the chelating property of the DOTA structure. By changing the amines and the basic structure of the system, many different combinations can be prepared and studied in a single screening assay with the agents attached to the solid support, a much easier way than the conventional solution-phase practices. This parallel synthesis method can, in principle, be used to create diverse libraries of MRI or PET agents for protein and cell targeting purposes. Thousands of different amines are commercially available to bring the ligand diversity. Today, high-throughput parallel synthesizers are also commercially available, making these studies even easier to apply. Upon use of these automated synthesizers, the diversity can be applied to all four arms of DOTA scaffold equally, and thereby near symmetrical and even much larger DOTA libraries can be synthesized in the future. Nonetheless, the best compounds we isolated in this study can also be synthesized with full symmetry in the solution phase for practical applications as better CEST agents. Studies are being continued to validate these compounds further in both in vitro and in vivo applications.

■ ASSOCIATED CONTENT

ⓈSupporting Information. Detailed experimental procedures, chemical structure of compound **16** (CNBr cleaved form), spectral data (MALDI-MS, HPLC) of compound **16** and the library, and complete ref 29. This material is available free of charge via the Internet at http://pubs.acs.org.

■ AUTHOR INFORMATION

Corresponding Author
E-mail: gomika.udugama@utsouthwestern.edu.

■ ACKNOWLEDGMENT

■ REFERENCES

(1) Terreno, E.; Dastru, W.; Delli Castelli, D.; Gianolio, E.; Geninatti Crich, S.; Longo, D.; Aime, S. *Curr. Med. Chem.* **2010**, *17*, 3684–3700.

(2) Hancu, I.; Dixon, W. T.; Woods, M.; Vinogradov, E.; Sherry, A. D.; Lenkinski, R. E. *Acta Radiol.* **2010**, *51*, 910–923.

(3) Wu, Y.; Soesbe, T. C.; Kiefer, G. E.; Zhao, P.; Sherry, A. D. *J. Am. Chem. Soc.* **2010**, *132*, 14002–14003.

(4) Wu, Y.; Zhao, P.; Kiefer, G. E.; Sherry, A. D. *Macromolecules* **2010**, *43*, 6616.

(5) Sherry, A. D.; Woods, M. *Annu. Rev. Biomed. Eng.* **2008**, *10*, 391–411.

(6) Woods, M.; Woessner, D. E.; Sherry, A. D. *Chem. Soc. Rev.* **2006**, *35*, 500–511.

(7) Zhang, S.; Merritt, M.; Woessner, D. E.; Lenkinski, R. E.; Sherry, A. D. *Acc. Chem. Res.* **2003**, *36*, 783–790.

(8) Ward, K. M.; Aletras, A. H.; Balaban, R. S. *J. Magn. Reson.* **2000**, *143*, 79–87.

(9) Vinogradov, E.; He, H.; Lubag, A.; Balschi, J. A.; Sherry, A. D.; Lenkinski, R. E. *Magn. Reson. Med.* **2007**, *58*, 650–655.

(10) Liu, G.; Ali, M. M.; Yoo, B.; Griswold, M. A.; Tkach, J. A.; Pagel, M. D. *Magn. Reson. Med.* **2009**, *61*, 399–408.

(11) Zhao, J. M.; Har-el, Y. E.; McMahon, M. T.; Zhou, J.; Sherry, A. D.; Sgouros, G.; Bulte, J. W.; van Zijl, P. C. *J. Am. Chem. Soc.* **2008**, *130*, 5178–5184.

(12) Ling, W.; Regatte, R. R.; Navon, G.; Jerschow, A. *Proc. Natl. Acad. Sci. U.S.A.* **2008**, *105*, 2266–2270.

(13) McMahon, M. T.; Gilad, A. A.; Zhou, J.; Sun, P. Z.; Bulte, J. W.; van Zijl, P. C. *Magn. Reson. Med.* **2006**, *55*, 836–847.

(14) Zhang, S.; Sherry, A. D. *J. Solid State Chem.* **2003**, *171*, 38–43.

(15) Liu, G.; Gilad, A. A.; Bulte, J. W.; van Zijl, P. C.; McMahon, M. T. *Contrast Media Mol. Imaging* **2010**, *5*, 162–170.

(16) McMahon, M. T.; Gilad, A. A.; DeLiso, M. A.; Berman, S. M.; Bulte, J. W.; van Zijl, P. C. *Magn. Reson. Med.* **2008**, *60*, 803–812.

(17) Olivos, H. J.; Alluri, P. G.; Reddy, M. M.; Salony, D.; Kodadek, T. *Org. Lett.* **2002**, *4*, 4057–4059.

(18) Simpson, L. S.; Burdine, L.; Dutta, A. K.; Feranchak, A. P.; Kodadek, T. *J. Am. Chem. Soc.* **2009**, *131*, 5760–5762.

(19) Zuckermann, R. N.; Kerr, J. M.; Kent, S. B. H.; Moos, W. H. *J. Am. Chem. Soc.* **1992**, *114*, 10646–10647.

(20) De Silva, C. R.; Vagner, J.; Lynch, R.; Gillies, R. J.; Hruby, V. J. *Anal. Biochem.* **2010**, *398*, 15–23.

(21) Handl, H. L.; Vagner, J.; Yamamura, H. I.; Hruby, V. J.; Gillies, R. J. *Anal. Biochem.* **2005**, *343*, 299–307.

(22) Dixon, W. T.; Ren, J.; Lubag, A. J.; Ratnakar, J.; Vinogradov, E.; Hancu, I.; Lenkinski, R. E.; Sherry, A. D. *Magn. Reson. Med.* **2010**, *63*, 625–632.

(23) Mani, T.; Tircso, G.; Togao, O.; Zhao, P.; Soesbe, T. C.; Takahashi, M.; Sherry, A. D. *Contrast Media Mol. Imaging* **2009**, *4*, 183–191.

(24) Viswanathan, S.; Ratnakar, S. J.; Green, K. N.; Kovacs, Z.; De Leon-Rodriguez, L. M.; Sherry, A. D. *Angew. Chem., Int. Ed.* **2009**, *48*, 9330–9333.

(25) Alluri, P. G.; Reddy, M. M.; Bachhawat-Sikder, K.; Olivos, H. J.; Kodadek, T. *J. Am. Chem. Soc.* **2003**, *125*, 13995–14004.

(26) Udugamasooriya, D. G.; Dineen, S. P.; Brekken, R. A.; Kodadek, T. *J. Am. Chem. Soc.* **2008**, *130*, 5744–5752.

(27) Udugamasooriya, D. G.; Dunham, G.; Ritchie, C.; Brekken, R. A.; Kodadek, T. *Bioorg. Med. Chem. Lett.* **2008**, *18*, 5892–5894.

(28) Zuckermann, R. N.; Kodadek, T. *Curr. Opin. Mol. Ther.* **2009**, *11*, 299–307.

(29) Simon, R. J.; et al. *Proc. Natl. Acad. Sci. U.S.A.* **1992**, *89*, 9367–9371.

(30) Kwon, Y. U.; Kodadek, T. *J. Am. Chem. Soc.* **2007**, *129*, 1508–1509.

(31) Astle, J. M.; Udugamasooriya, D. G.; Smallshaw, J. E.; Kodadek, T. *Int. J. Pept. Res. Ther.* **2008**, *14*, 223–227.